NON-INVASIVE BEAM PROFILE MEASUREMENT FOR HIGH INTENSITY ELECTRON BEAMS

T. Weilbach, M. Bruker, Helmholtz-Institut Mainz, Germany,
K. Aulenbacher, KPH Mainz, Helmholtz-Institut Mainz, Germany

Abstract

Beam profile measurements of high intensity electron beams below 10 MeV, e.g. in energy recovery linacs or magnetized high energy electron coolers, have to fulfill special demands. Commonly used diagnostic tools like synchrotron radiation and scintillation screens are ineffective or not able to withstand the beam power without being damaged. Non-invasive methods with comparable resolution are needed.

Hence, a beam profile measurement system based on beam-induced fluorescence (**BIF**) was built. This quite simple system images the light generated by the interaction of the beam with the residual gas onto a PMT. A more elaborated system, the Thomson Laser Scanner (**TLS**) — the non-relativistic version of the Laser Wire Scanner — is proposed as a method for non-invasive measurement of all phase space components, especially in the injector and merger parts of an ERL. Since this measurement suffers from low count rates, special attention has to be given to the background.

Beam profile measurements with the BIF system will be presented as well as a comparison with YAG screen measurements. The recent status of the TLS system will be presented.

INTRODUCTION

High-intensity electron beams are getting more and more popular. Because of their high beam power, the use of conventional destructive diagnostic tools is limited. Energy recovery linacs (ERL) can make use of the emitted synchrotron radiation for profile measurements, but this is only possible after the main linac. In the injector and merger section, they need non-intercepting beam diagnostic devices which can withstand the beam power of several 100 kW. The planned electron cooling devices easily reach several MW of beam power. Because of energy recuperation in the collector, they allow only a very small beam loss, which is not compatible with normal destructive diagnostics.

There are already several non-destructive beam diagnostic methods established, which are used in different accelerators, such as a scintillation profile monitor [1] at COSY or the laser wire scanner at the synchrotron source PETRA III [2]. These methods can be adapted for the profile measurement of high-intensity electron beams with energies in the MeV range.

EXPERIMENTAL SETUP

All measurements are done at the polarized test source (PKAT) [3] shown in Fig. 1 at the Mainzer Mikrotron (MAMI). In this source, a NEA-GaAs [4] photo cathode is used to generate an electron beam with an energy of 100 keV.
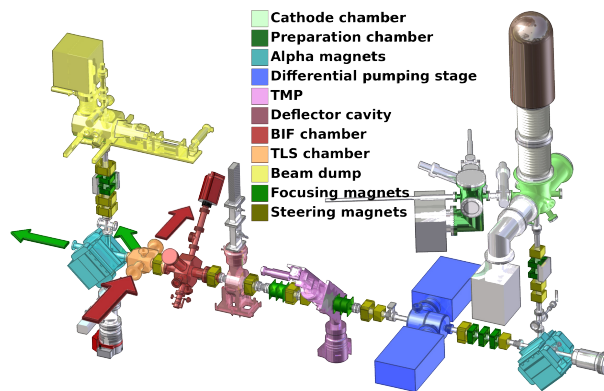

Figure 1: The polarized test source PKAT. The first differential pumping stage (blue) separates the source vacuum (green) from the beam line vacuum. A second differential pumping stage (purple) separates the BIF (red) and the TLS chamber (orange) from the rest of the beam line. The Faraday cup (yellow) monitors the beam current throughout the measurements.

The NEA-GaAs cathode requires a pressure much lower than 10^{-10} mmbar for stable operation. Therefore, a first differential pumping stage separates the source vacuum from the beam line vacuum (blue). A second differential pumping stage, consisting of two turbo molecular pumps (purple), surrounds the BIF and TLS chambers. This allows local pressure bumps of up to 10^{-5} mbar while maintaining the UHV condition at the cathode.

The beam transport system consists of dipole (alpha and steering magnets) and quadrupole magnets as well as two solenoid doublets. Several conventional (luminescent and scintillating) screens and the Faraday cup at the end of the beam line allow for a setup of the electron beam and also for comparison measurements with the new non-invasive diagnostic methods.

The PKAT can operate in several modes which differ in the time structure of the electron beam. For the BIF measurements, we use the dc mode, in which a blue laser diode generates either a dc beam or a pulsed beam with a repetition rate of several Hz with a length of a few 100 µs. In that mode, the source is limited to 500 µA.

For the TLS measurements, a larger current is needed. Since the power supply can only provide 3 mA of dc current, a pulsed system with a pulse length of about 20 ns and a rep. rate of 150 kHz was built. Thus the PKAT can create an electron beam with a peak current of 30 mA while the average current is approximately 90 µA. The red arrows in Fig. 1 show the incident laser while the green arrows show
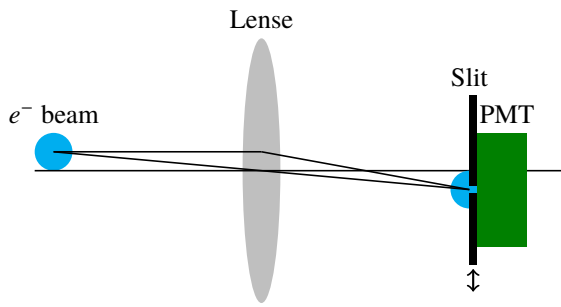
Figure 2: Schematic view of the beam induced fluorescence profile measurement done with a PMT and a slit. The light created by the energy loss of the electron beam is imaged with a lens onto a PMT. A moving slit in front of the PMT provides the spatial resolution needed for profile measurements.

Table 1: Typical BIF Profile Measurement Conditions

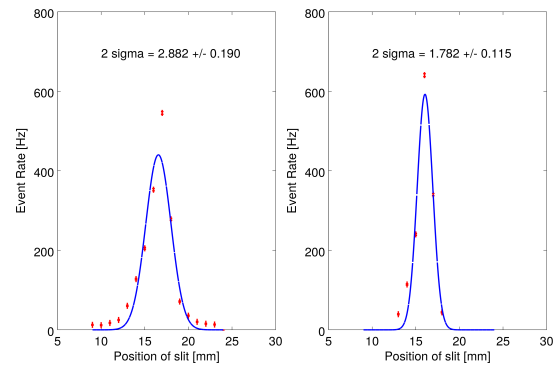|	
Beam energy	100 keV
Beam current	100 µA
Residual gas pressure	$\approx 10^{-5}$ mbar
PMT voltage	1000 V
Slit width	0.2 mm

Figure 3: BIF measurement with statistical errors with different focusing strengths of the solenoid in front of the BIF chamber. The measurement is shown in red and the Gaussian fit in blue. Left: Solenoid current 50 mA, right: Solenoid current 500 mA.
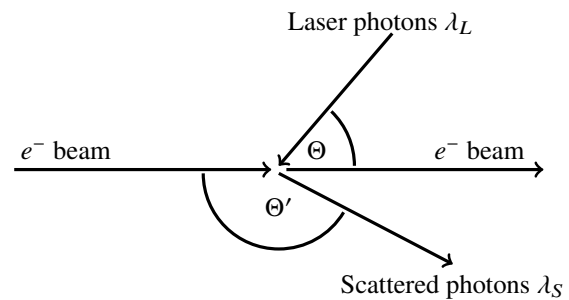

Figure 4: Thomson scattering scheme. The angle between electron beam and incident laser beam is Θ while Θ' is the angle between the electron beam and the scattered photons.

the two possible detector positions for the measurement of the scattered photons.

BEAM-INDUCED FLUORESCENCE

For protons and ions, beam profile measurement based on beam-induced fluorescence is a common technique [5]. The idea is to image the fluorescing residual gas on a photo detector with a spatial resolution. Instead of a detector with a spatial resolution, a photomultiplier tube (PMT) with a slit in front of it can be used. The slit cuts out a small slice of the electron beam image at the PMT as indicated in Fig. 2. By moving the slit up and down and measuring the photon intensity, a beam profile can be measured.

The intensity of the photons is proportional to the pressure and the beam current. As stated above, the current is limited so the only possibility to enhance the signal is to raise the residual gas pressure. A gas dosing valve is used to insert N_2 gas in the vacuum system. Nitrogen converts 3.6 keV of average energy loss into one visible photon [6]. The energy loss of the electron beam can be calculated with a modified form of the Bethe-Bloch formula. Another advantage of N_2 is that it can be pumped out of the vacuum system very easily. Therefore, residual gas pressures of 10^{-5} mbar can be generated in the BIF chamber without destroying other parts of the apparatus. Table 1 shows the typical conditions during a measurement.

Figure 3 shows typical experimental results. The PMT is used in the counting mode with a discriminator and a rate meter. The rate is measured with respect to the slit position. In this measurement, the beam current was 75 µA and the focus of the beam was changed with the solenoid in front

of the BIF chamber. The width of the beam changes due to the changing focusing strength of the solenoids. A Gaussian function (blue) is fitted to the measured values including statistical errors (red) to extract the beam width.

THOMSON SCATTERING

Thomson scattering describes elastic scattering of a photon on a free electron. It is the low-energy limit of the Compton scattering process. Fig. 4 shows a schematic view of Thomson scattering.

A photon λ_L hits the electron beam with an angle Θ and is scattered with the scattering angle Θ'. The scattered photon λ_S gains energy due to the Doppler shift. The wavelength of the scattered photon as a function of the angle between incident photon and electron and the angle between scattered photon and electron can be evaluated with

$$\lambda_S = \lambda_L \frac{(1 + \beta \cos \Theta')}{(1 + \beta \cos \Theta)} \qquad (1)$$

where β is the electron velocity in units of the speed of light. The number of scattered photons can be calculated with the following equation:
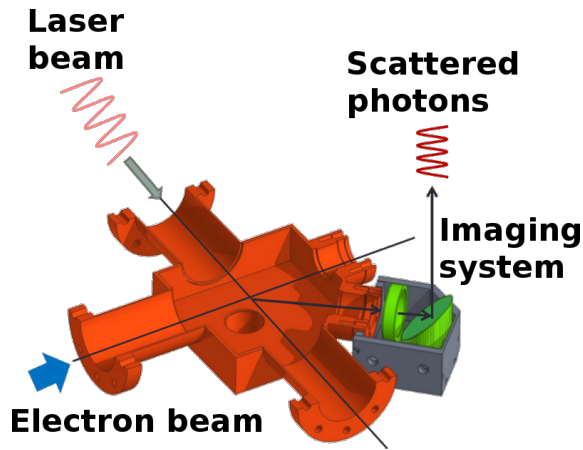
Figure 5: Half section of the TLS chamber (orange) and the detector system. The angle between laser and electron beam is $\Theta = 90°$ whereas $\Theta' = 135°$ is the angle between electron beam and scattered photons. The imaging system (green) consists of a lens and a parabolic mirror.

$$R = \frac{1}{2}r_e^2 \left(1 + \cos^2\Theta'\right) N_L n_e P \epsilon \Delta\Omega l \frac{(1 + \beta\cos(\Theta))}{(1 + \beta\cos(\Theta'))\gamma} \quad (2)$$

with r_e = classical electron radius, N_L = number of incident photons per Joule, n_e = electron density, P = laser power, ϵ = detector system efficiency, $\Delta\Omega$ = detector solid angle, l = interaction length, $\frac{(1+\beta\cos(\Theta))}{(1+\beta\cos(\Theta'))\gamma}$ = factor resulting from Lorentz transformation.

For our experiment, we are using the following angles: $\Theta = 90°$ and $\Theta' = 135°$. With an electron energy of 100 keV, a current of 25 mA, $P = 130$ W, $\epsilon = 0.17$, $\Delta\Omega = 0.01$, $l = 3$ mm (beam diameter) the expected rate is about 5 Hz.

The rate of the scattered photons is proportional to the integrated electron density along the path of the laser through the electron beam (calculations were made for a homogeneously charged electron beam while the laser passes the center). By moving the laser beam through the electron beam vertically, a profile measurement can be done. Due to the low cross section, which is mostly dominated by the classical electron radius squared, the required laser power is very high. This was the reason why the pioneer experiment done in 1987/88 suffered from very low count rates [7]. Figure 5 shows a half section of the CAD-model of the TLS chamber. The paths of the electron beam, the incident Laser beam, and the scattered photons are indicated. Due to the limited space, the detector cannot be placed in the scattering plane. Therefore, an imaging system consisting of a lens and a parabolic mirror images the interaction region onto the PMT passing two bandpass filters that reduce the background created by the laser.

Since we are using a pulsed electron beam and a pulsed laser system, the synchronization of both has to be guaranteed.
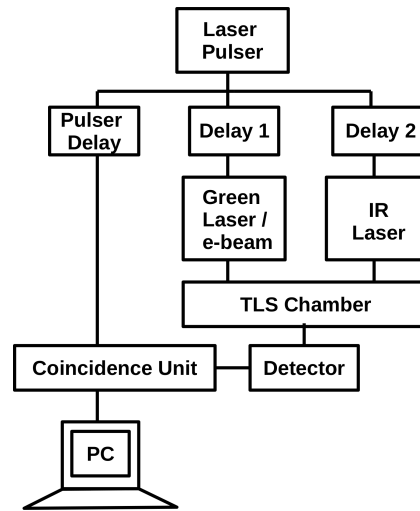

Figure 6: Schematic diagram of the synchronization system. The pulser delay as well as delay 1 and delay 2 can be changed individually to achieve a synchronous arrival of the electron beam, which is generated by the green laser, and the IR laser beam at the interaction point.

Synchronization

To ensure a simultaneous arrival of the laser and the electron beam, an elaborated synchronization scheme has been built. This is shown in Fig. 6. The common time base is the laser pulser which triggers all following elements. The pulser delay is used for the coincidence unit while delay 1 and delay 2 compensate for the time of flight of the electron beam. Thus with the right delays, a synchronization of the electron beam and the laser can be guaranteed as shown in Fig. 7.

The most important laser properties are given in Tab. 2. The high power of the IR laser can be used for the synchronization of the apparatus. While the photons pass the vacuum window, a few of them get scattered and have their wavelengths shifted to the transmission band of the bandpass filters so they are detectable with the PMT. For the TLS measurement, the photon background caused by this is a problem but the signal can be used for the adjustment of the delay lines (Fig. 7, red points). To obtain a correct timing of the electron beam signal, we caused a beam loss in the TLS chamber in front of the detector. This also creates photons with different wavelengths so some of them are able to reach the detector (Fig. 7, black points). In contrast to the IR signal, the signal generated by the beam loss can be reduced or even made to disappear for a good optics setup of the beam line.

Background Reduction

Different background sources have been identified, such as ambient light from the lab that enters through vacuum windows, or even pressure sensors which are installed in the PKAT [8]. One can get rid of most of these sources by a sufficient shielding of the detector system or switching

Table 2: TLS Laser System Properties

IR laser power	130 W
IR wavelength	1030 nm
IR pulse length	16 ns
Green laser power	11 W
Green wavelength	515 nm
Green pulse length	19 ns
Rep. rate	150 kHz

Figure 8: Different IR background levels for different experimental setups. The IR background in the initial chamber (red), with additional blackened tubes (black) and with the new blackened and improved chamber (blue). The vertical movement of the laser is generated by a system of moving mirrors, i.e. the mirror position represents the laser position during the scanning process. The hot spot at 14 mm is reproducible, very narrow (less than 1 mm), and seems to be an impurity of the vacuum window.
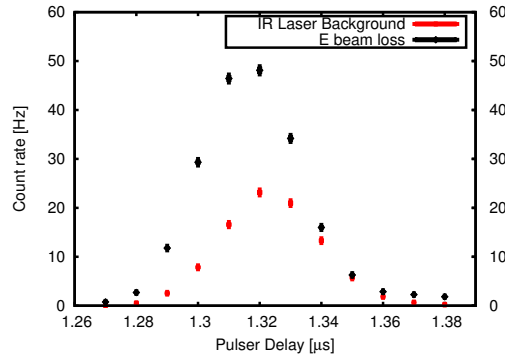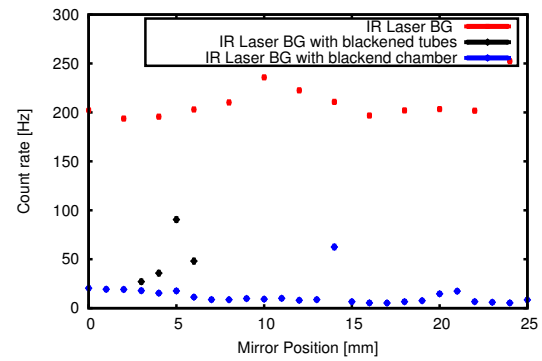

Figure 7: Measurement of the background signal caused by the IR laser and the measurement of the beam loss of the electron beam in the TLS chamber. The delay lines are adjusted so that both signals overlap each other to ensure a simultaneous arrival of both beams.

them off like the pressure sensor. Furthermore, if these sources generate light in a dc manner, the background is suppressed due to the duty cycle of the pulsed laser system and the coincidence unit by a factor of about 350. The biggest problem is the beam-correlated background, which is not suppressed. The two most important sources for that are electron beam loss and the IR laser itself. First measurements have shown that the electron beam loss can be held on a level of a few Hz with a proper adjustment of the beam optics [9]. The IR background however is more complicated to reduce and is higher than the electron beam loss. Figure 8 shows the results of several measurements. The first measurement (red) shows the initial conditions. The background was well above 200 Hz, making TLS profile measurement very time consuming if not impossible. A first improvement was the insertion of two blackened pipes in the vacuum chamber. This reduced the background by the IR laser by a factor of 3 to 4 (black). Unfortunately, after the fourth measured point the laser broke down, so no further measurements were possible. Therefore, we designed a new TLS chamber where the vacuum window has no direct line of sight to the detector system. In addition, two apertures were introduced into the chamber to reduce the solid angle of the photons scattered by the windows. Finally, the whole chamber was blackened on the inside to absorb stray light. The third curve (blue) shows the huge impact on the background which was achieved. The background is below 10 Hz nearly at every mirror position, so that TLS profile measurements are now possible. The vertical movement of the laser is generated by a system of

moving mirrors, i.e. the mirror position represents the laser position during the scanning process.

OUTLOOK

For comparison measurements a YAG screen is also installed in the BIF chamber and measurements with BIF and YAG are planned for the near future. Since the Background for the TLS measurement seems to be under control the final profile measurement will be carried out soon.

REFERENCES

[1] C. Boehme et al., "Gas Scintillation Beam Profile Monitor at COSY Jülich", TUPSM005, Proceedings of BIW 2010, Santa Fe, New Mexico USA.

[2] M.T. Price et al., "Beam Profile Measurements with the 2-D Laser-Wire Scanner at PETRA", FRPMN094, Proceedings of PAC 2007, Albuquerque, New Mexico USA.

[3] P. Hartmann: "Aufbau einer gepulsten Quelle polarisierter Elektronen", Dissertation 1997, JGU Mainz, Germany

[4] D.T. Pierce et al., Appl. Phys. Lett. 26 (1975) 670.

[5] F. Becker, "Beam Induced Fluorescence Monitors", WEOD01, Proceedings of DIPAC 2011, Hamburg, Germany.

[6] M.A. Plum et al., Nucl. Instr. Meth. A 492 (2002), p. 74.

[7] C. Habfast et al., "Measurement of Laser Light Thomson-Scattered from a Cooling Electron Beam", Appl. Phys. B 44, 87-92 (1987).

[8] T. Weilbach et al.: Optical Electron Beam Diagnostics for Relativistic Electron Cooling Devices, Proceedings of COOL 11, Alushta, Ukraine, 2011.

[9] K. Aulenbacher et al.: Exploring New Techniques for Operation and Diagnostics of Relativistic Electron Coolers, Proceedings of COOL 15, Newport News, Virginia, USA, 2015.